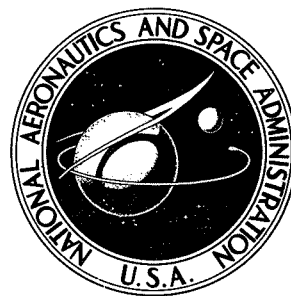


NASA TECHNICAL NOTE



NASA TN D-7360

NASA TN D-7360

ACOUSTIC RADIATION PATTERNS FOR A SOURCE IN A HARD-WALLED UNFLANGED CIRCULAR DUCT

by Raymond G. Holm and William E. Zorumski

Langley Research Center

Hampton, Va. 23665

1. Report No. NASA TN D-7360	2. Government Accession No.	3. Recipient's Catalog No.	
4. Title and Subtitle ACOUSTIC RADIATION PATTERNS FOR A SOURCE IN A HARD-WALLED UNFLANGED CIRCULAR DUCT		5. Report Date November 1973	6. Performing Organization Code
		8. Performing Organization Report No. L-9025	10. Work Unit No. 501-24-01-01
7. Author(s) Raymond G. Holm and William E. Zorumski		11. Contract or Grant No.	
		13. Type of Report and Period Covered Technical Note	
9. Performing Organization Name and Address NASA Langley Research Center Hampton, Va. 23665		14. Sponsoring Agency Code	
		12. Sponsoring Agency Name and Address National Aeronautics and Space Administration Washington, D.C. 20546	
15. Supplementary Notes			
16. Abstract Acoustic radiation patterns are measured over a 320° arc for a point source in a finite-length, hard-walled, unflanged circular duct. The measured results are compared with computed results which are based on the Wiener-Hopf solution for radiation from a semi-infinite unflanged duct. Measurements and computations are presented for frequencies slightly below and slightly above each of the first four higher-order radial mode cut-off frequencies. It is found that the computed and measured patterns show better agreement below the mode cut-off frequencies than above and that the agreement is better at lower frequencies than at higher frequencies. The computed radiation patterns do not show fine lobes which are caused by diffraction from the back end of the duct.			
17. Key Words (Suggested by Author(s)) Acoustic radiation Duct radiation		18. Distribution Statement Unclassified - Unlimited	
19. Security Classif. (of this report) Unclassified	20. Security Classif. (of this page) Unclassified	21. No. of Pages 18	22. Price* Domestic, \$2.75 Foreign, \$5.25

ACOUSTIC RADIATION PATTERNS FOR A SOURCE IN A HARD-WALLED UNFLANGED CIRCULAR DUCT

By Raymond G. Holm and William E. Zorumski
Langley Research Center

SUMMARY

Acoustic radiation patterns are measured for a source in a hard-walled unflanged circular duct. The duct is of the form of a short barrel (length = diameter) with a point source of sound in the center of its closed end. Acoustic radiation patterns are measured in the angular range 0° to $\pm 160^\circ$ from the duct axis at frequencies just above and just below the cut-off frequencies of the first four higher-order radial duct modes. The measured radiation patterns are compared with computed patterns which are based on the Wiener-Hopf solution for radiation from a semi-infinite unflanged duct. Measurements are also made of the far-field sound pressure level as a function of frequency at several angles.

The measurements of sound pressure level as a function of frequency show sudden changes of up to 20 dB at the duct mode cut-off frequencies. The measured radiation patterns above and below the cut-off frequencies are also significantly different. The computed radiation patterns are in fair agreement with the measured patterns. In general, the agreement is better below the mode cut-off frequencies than above and is better at lower frequencies than at higher frequencies. The measured radiation patterns show many fine lobes which are caused by diffraction from the back end of the duct, whereas the computed patterns do not have lobes in this angular range.

INTRODUCTION

The radiation of sound from a circular waveguide is an acoustical problem which must be considered in a number of practical situations. Two mathematical models have been used in the study of this problem. These models are (1) the duct with an infinite rigid flange and (2) the unflanged duct.

Morse (ref. 1) has derived equations for the radiation impedance of a hard-walled circular duct with an infinite rigid flange and has made a short table of these radiation impedances. Morse shows how the method of successive approximations may be used, once the mode radiation impedances are known, to calculate radiation from the flanged circular duct. In reference 2, Morse's results are extended to the case of annular ducts

with acoustically treated walls and it is shown that the radiation impedances may be used (in a set of linear equations) to find the sound field inside the duct (due to a source inside the duct) and the radiated sound field.

The mathematical problem of radiation from a semi-infinite unflanged circular duct is a mixed boundary-value problem which can be solved by the Wiener-Hopf technique which is discussed in reference 3. This solution for radiation from an unflanged circular duct with higher-order radial and circumferential acoustic modes is given in reference 4.

The purpose of this paper is to compare measured radiation patterns with theoretical patterns for an unflanged circular duct. A point acoustic source is used inside the duct since it is easy to represent this source mathematically and to create it experimentally.

The method of determining the sound field for this point source is given in reference 2 for the case of a flanged duct and the same analytical procedure is valid for the unflanged duct if unflanged duct reflection coefficients and radiation equations are used. The unflanged duct reflection coefficients and radiation directivity factors used in calculations in the present paper were obtained from reference 5.

APPARATUS AND PROCEDURES

A schematic illustration of the experiment is shown in figure 1. A source of sound originates inside the duct at the closed end, is transmitted to the front of the duct, and is then radiated outward where it is measured by the movable microphone. The boom microphone moves on an arc about the center of the duct opening and traverses a total angle of 320° .

The duct and its mathematical model are shown in figure 2. The duct (fig. 2(a)) is made of a double-walled reinforced steel shell which is packed with fiber glass to eliminate structural radiation. One end of the duct is closed with a heavy aluminum plate. A speaker is threaded into a small hole in the center of this plate to provide a point source of sound. The mathematical model of the duct (fig. 2(b)) is a semi-infinite circular duct with a rigid plate which is recessed a distance of 38.1 cm from the open end of the duct.

The duct assembly was mounted in an anechoic chamber with the assembly center line about 2 m above the floor grating so that grating reflections would be minimized. The temperature in the chamber was recorded so that the local sound speed could be calculated. A knowledge of this sound speed permitted selecting theoretically pertinent operating frequencies near the duct cut-off frequencies. Once a frequency was selected, the rotating boom was swept from 0° to $+160^\circ$ and then from 0° to -160° at a rate of $1.29^\circ/\text{sec}$. An attempt was made to synchronize the boom sweep rate with the sweep rate on a graphic level recorder used to polar-plot the output of the sweeping microphone. The microphone

signal was passed through a 50-Hz constant-bandwidth filter centered on the frequency recorded by the digital frequency meter. The microphone output was monitored on an oscilloscope to insure that the speaker was not being overdriven. Also, at specific polar angles (i.e., 0°, 20°, 40°, etc.), linear records were obtained of the sound-pressure-level (SPL) variation as the beat oscillator frequency was swept from 1000 Hz to 6000 Hz. These sweeps were made to demonstrate the sudden variations of radiated sound near the duct cut-off frequencies.

RESULTS AND DISCUSSION

The duct radial mode cut-off frequencies in terms of the product of wave number k times duct radius b are given in the following table:

Mode	kb	Cut-off frequency, Hz
0	0	0
1	3.83	1111
2	7.02	2037
3	10.17	2951
4	13.32	3865

These cut-off frequencies are calculated from the hard-walled duct boundary condition that the acoustic velocity normal to the duct wall is zero. This condition is expressed mathematically by the equation $J'_0(kb) = 0$, that is, the derivative of the Bessel function of the first kind of order zero is zero. The values in this table are based on a sound speed of 347.27 m/sec and a temperature of 26.9° C.

The directivity results obtained are presented in figures 3 to 10. The dotted theoretical curves accompany the experimental results with tick marks exterior to the polar grids to indicate the experimental 20° angular increments. Since the boom microphone and chart sweep rates were not precisely synchronized, there is distortion in the experimental angular scale.

The calculated sound pressure levels were matched to experimentally measured SPL's on axis (0°) in figures 3 to 10 by shifting the calculated values. This procedure was used because the actual sound power could not be controlled. The actual acoustic power radiated by the speaker could be determined analytically only from an extensive study of the speaker's dynamics, which is beyond the scope of the present paper.

A comparison of figures 3 and 4 shows that the radiation directivity pattern changes from below to above the cut-off frequency of the first higher-order radial duct mode.

Below the cut-off frequency, only the zeroth-order mode (plane wave) is propagating with the higher-order modes being exponentially attenuated. Above the cut-off frequency, the first higher-order mode propagates and, as predicted, dramatically enhances the axial and side-line sound radiation. Comparing figures 5 and 6, figures 7 and 8, and figures 9 and 10 shows similar features for the second, third, and fourth higher-order radial modes. In general, the agreement is better below the cut-off frequencies than above and better at lower frequencies than at higher frequencies. Many small lobes, which the analysis does not predict, are measured behind the plane of the duct opening. These small lobes are due to diffraction about the source end of the duct.

The sound-pressure-level variations at specific polar angles, as the speaker frequency was swept from 1000 Hz to 6000 Hz while maintaining the voltage to the speaker constant, are presented in figure 11. These graphs, particularly at sweeps of 20° and 80° , show a sudden increase in radiated sound pressure level as the frequency passes through a specific duct mode cut-off frequency. These results agree with the theoretical prediction that the power radiated from a constant volumetric strength source is infinite just above the cut-off frequencies of an infinite hard-walled duct.

CONCLUDING REMARKS

Acoustic radiation patterns have been measured and calculated for a source in a hard-walled circular duct without a flange. The measurements and calculations are in fair agreement; the agreement is better at lower frequencies. Theoretical predictions of sudden increases in side-line radiation as the frequency increases through a cut-off frequency are confirmed. The measured radiation patterns show a number of fine lobes behind the plane of the duct opening which are not predicted by theory. These lobes are caused by diffraction from the back end of the duct.

Langley Research Center,
National Aeronautics and Space Administration,
Hampton, Va., September 5, 1973.

REFERENCES

1. Morse, Philip M.: *Vibration and Sound*. Second ed., McGraw-Hill Book Co., Inc., 1948.
2. Zorumski, William E.: Generalized Radiation Impedances and Reflection Coefficients of Circular and Annular Ducts. *J. Acoust. Soc. Amer.*, vol. 54, no. 6, Dec. 1973.
3. Noble, B.: *Methods Based on the Wiener-Hopf Technique for the Solution of Partial Differential Equations*. Pergamon Press, Inc., c.1958.
4. Vajnshtejn, L. A. (J. Shmoys, transl.): *The Theory of Sound Waves in Open Tubes. Propagation in Semi-Infinite Waveguides*, Res. Rep. No. EM-63 (Contract No. AF-19(122)-42), Inst. Math. Sci., New York Univ., Jan. 1954, pp. 87-116.
5. Lansing, D. L.; Drischler, J. A.; and Pusey, C. G.: *Radiation of Sound From an Unflanged Circular Duct With Flow*. NASA paper presented at the 79th Meeting of the Acoustical Society of America (Atlantic City, N.J.), Apr. 21-24, 1970.

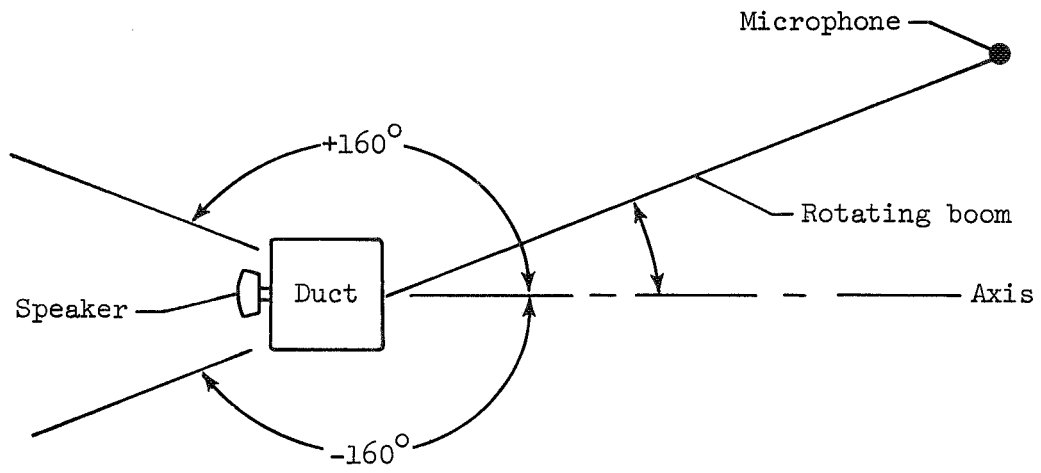
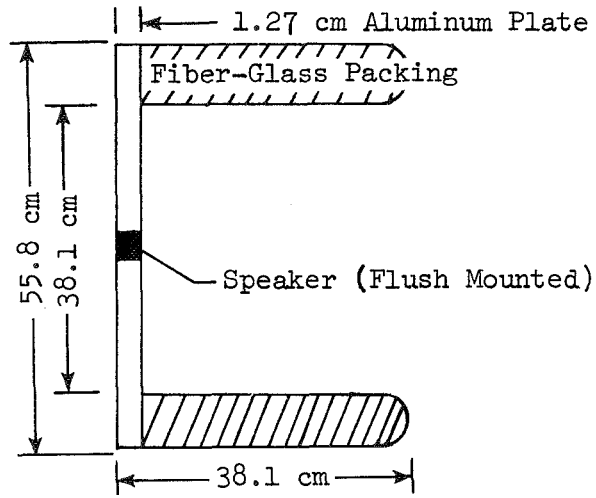
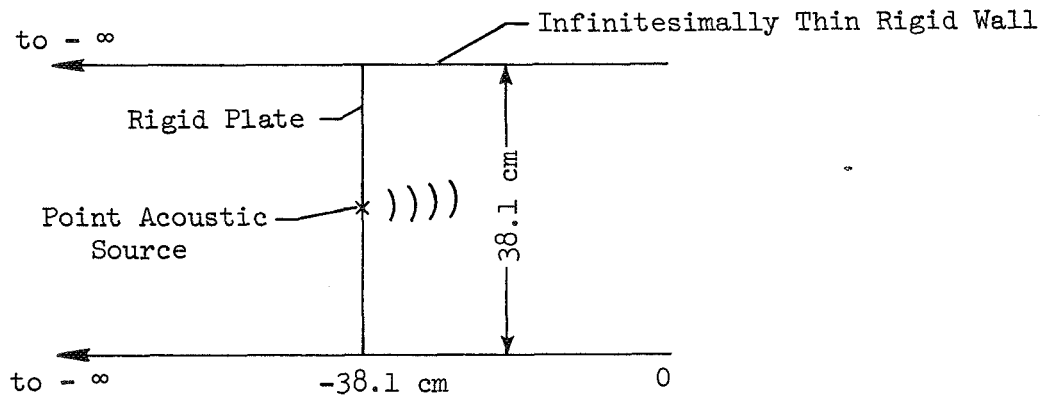


Figure 1.- Experiment schematic plan view.



(a) Experimental duct and speaker assembly.



(b) Mathematical model of duct with acoustic point source.

Figure 2. - Experimental duct and mathematical model.

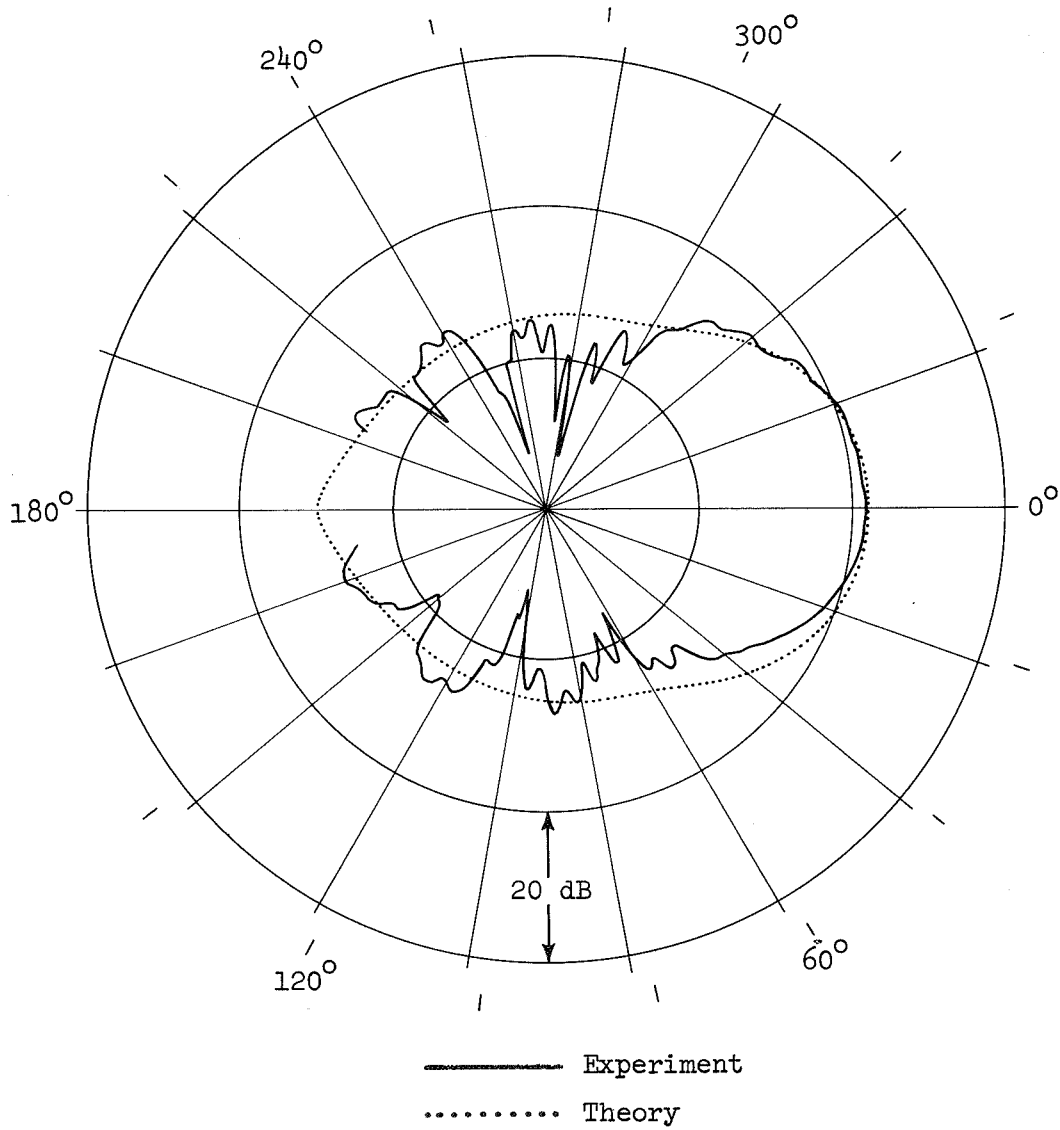


Figure 3.- Radiation patterns at 1082.5 Hz.

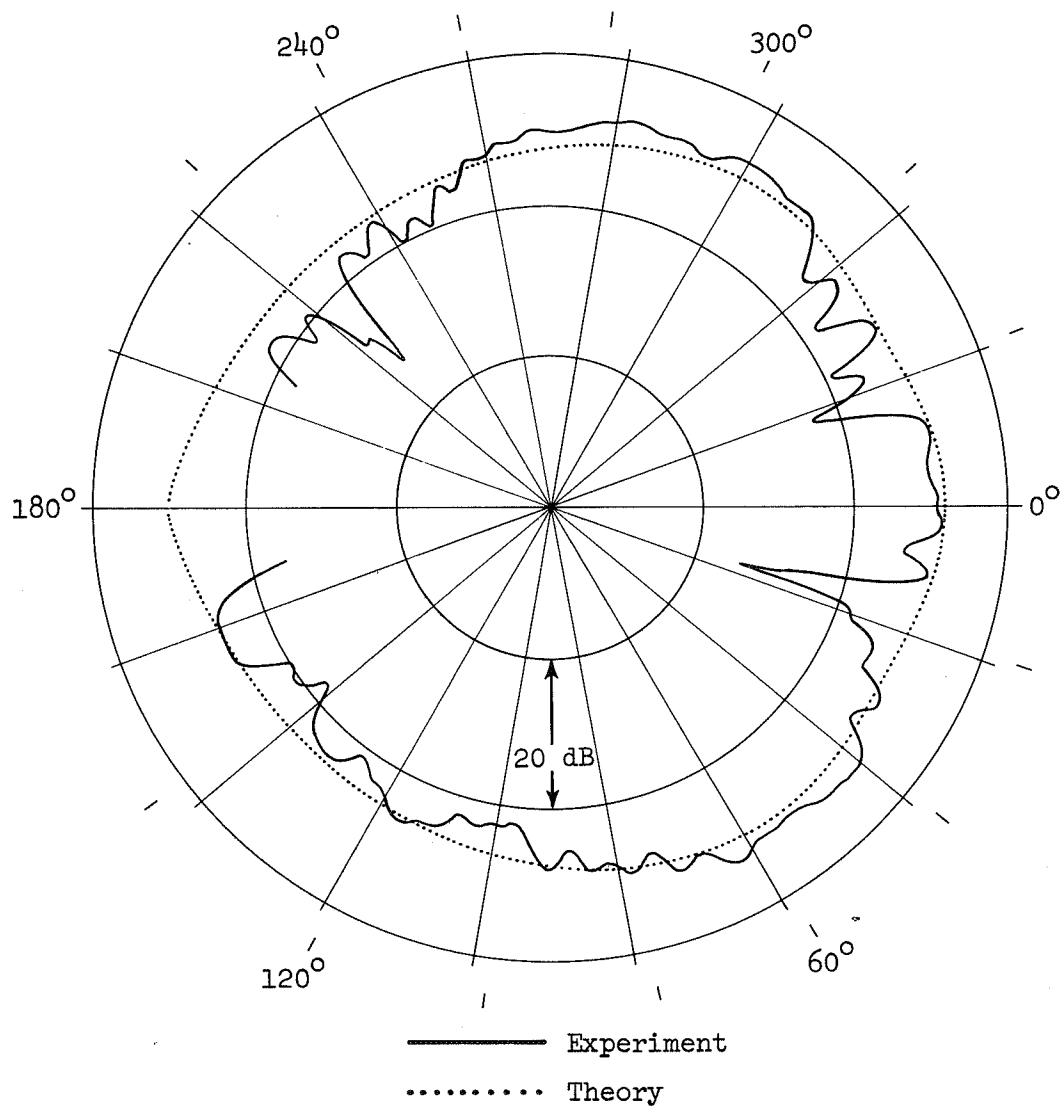


Figure 4.- Radiation patterns at 1133.1 Hz.

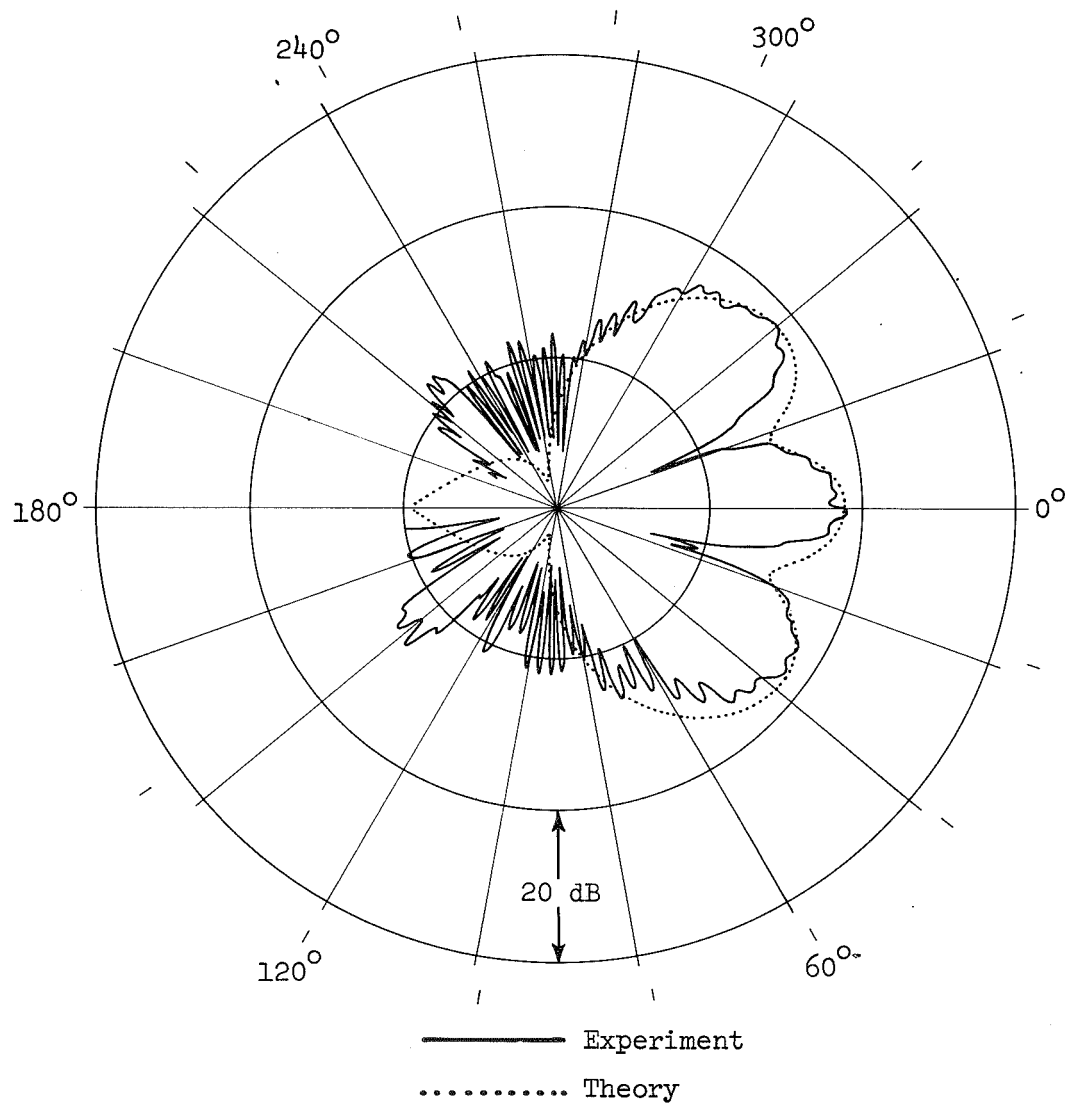


Figure 5.- Radiation patterns at 1998.2 Hz.

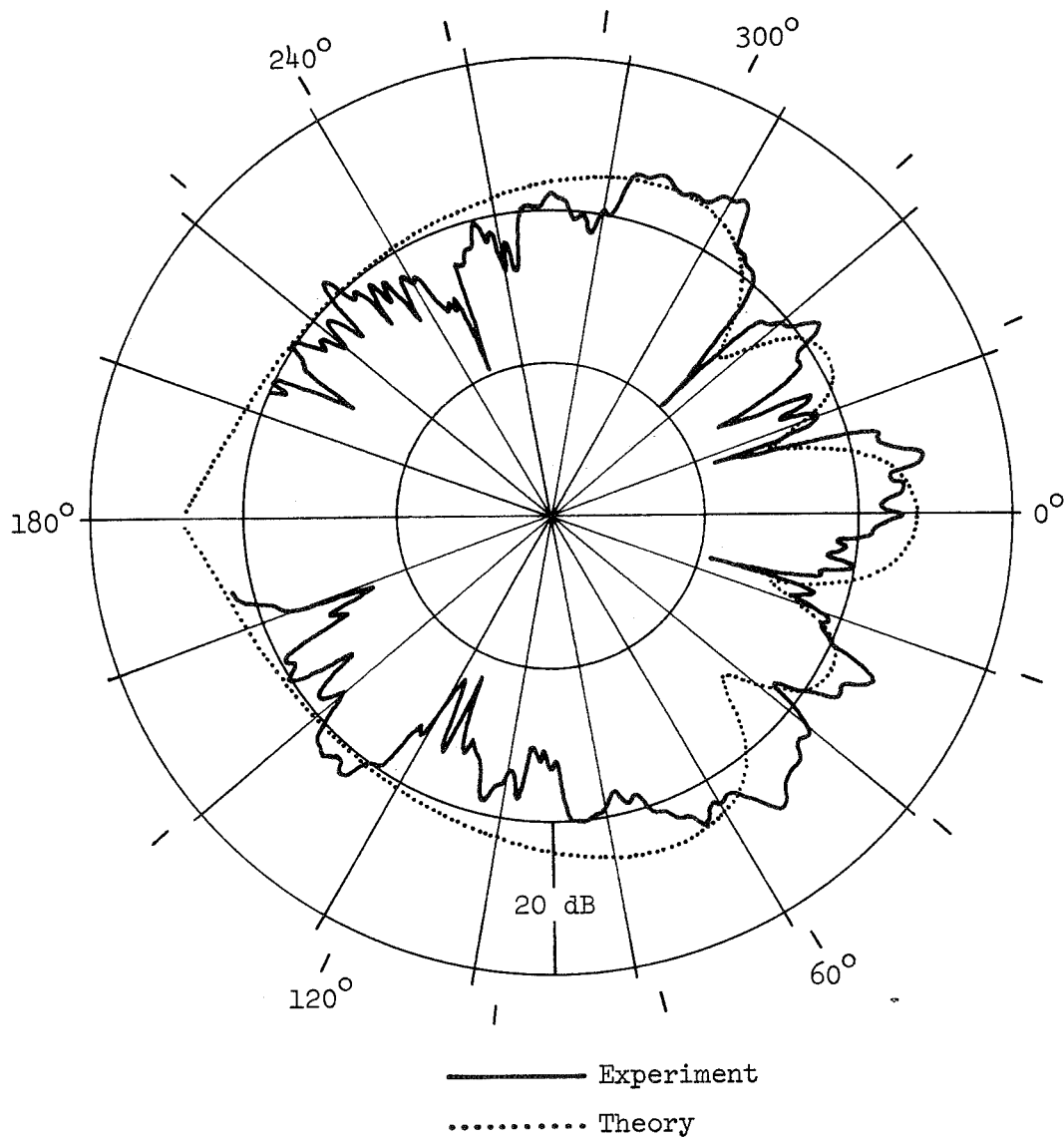


Figure 6.- Radiation patterns at 2058.9 Hz.

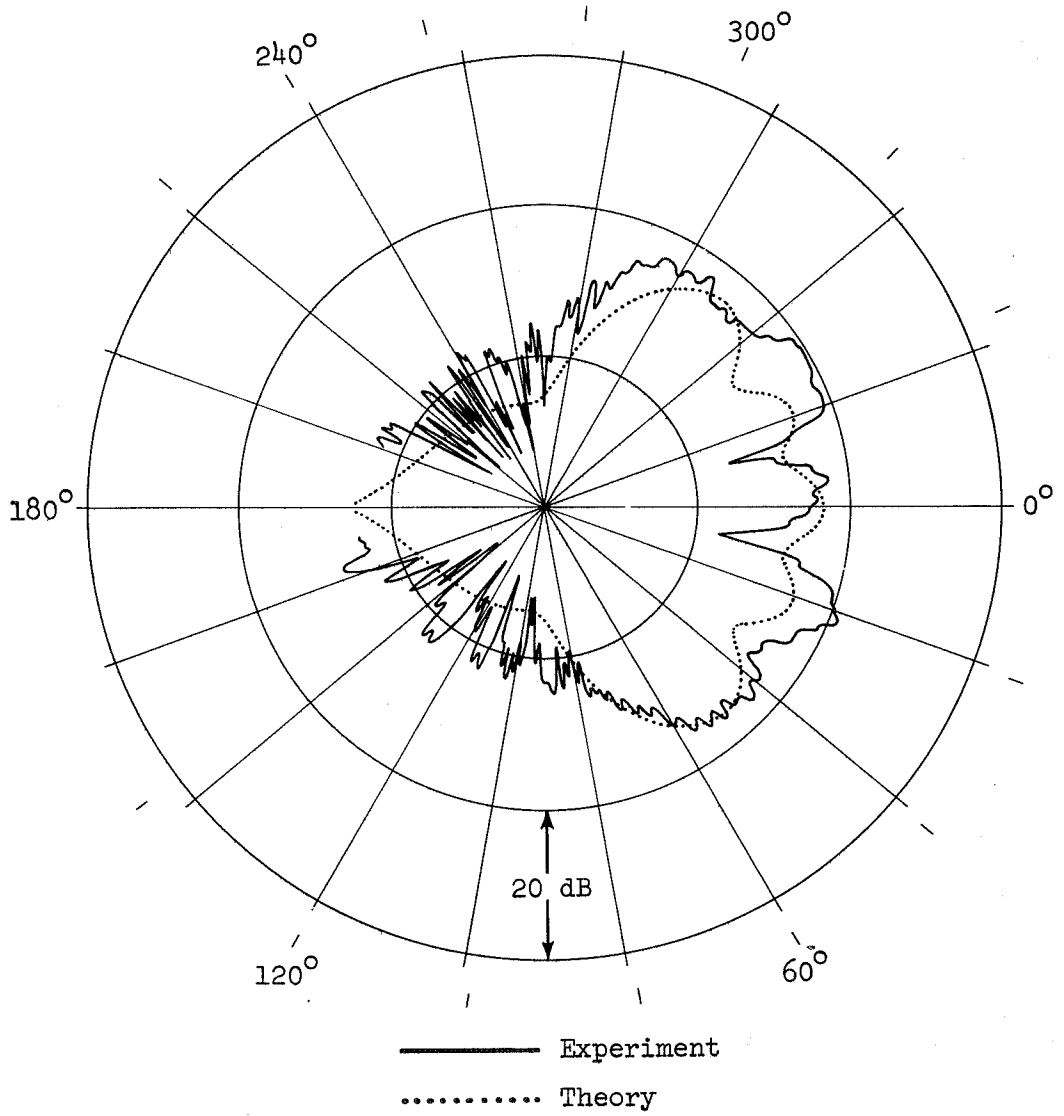


Figure 7.- Radiation patterns at 2883.1 Hz.

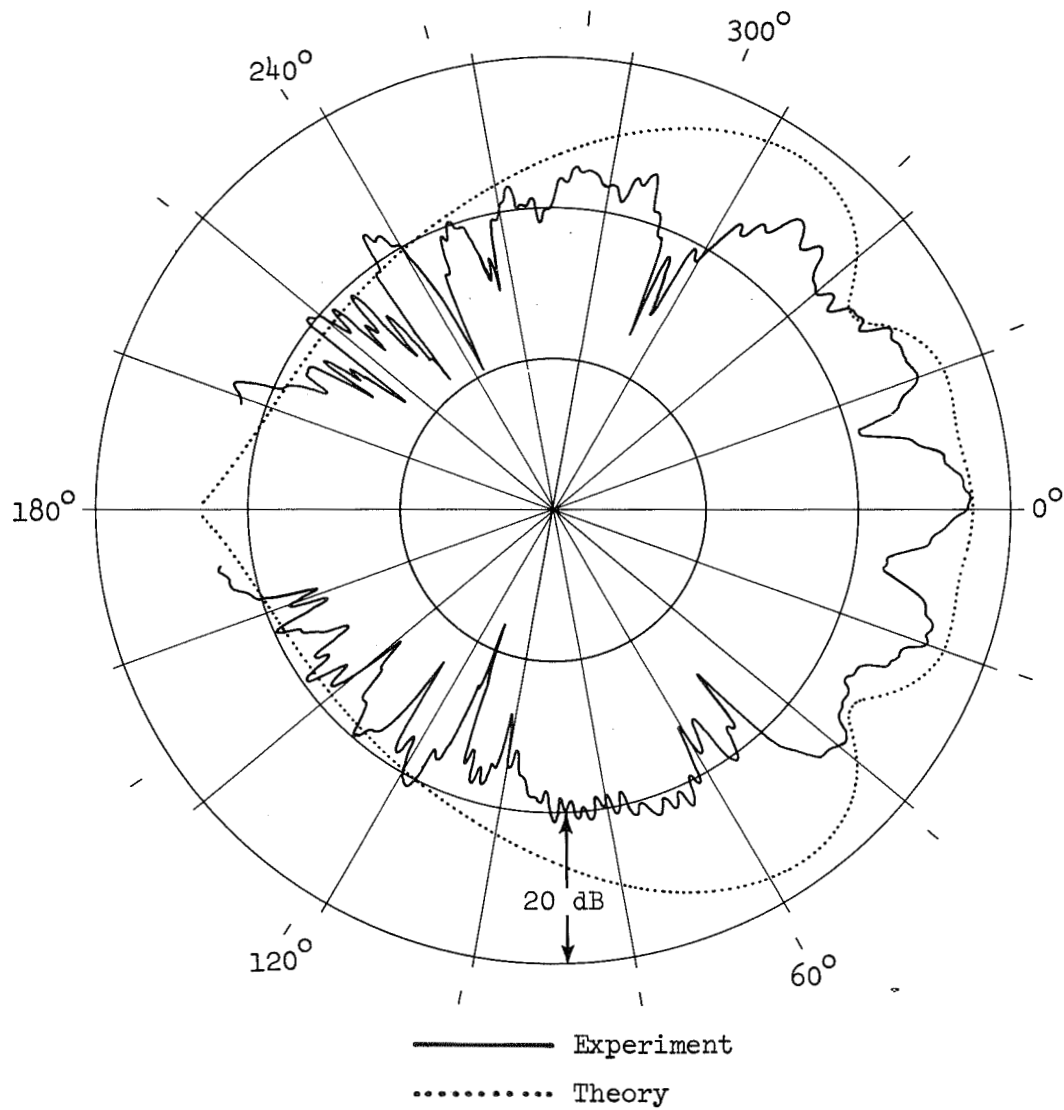


Figure 8.- Radiation patterns at 2977.8 Hz.

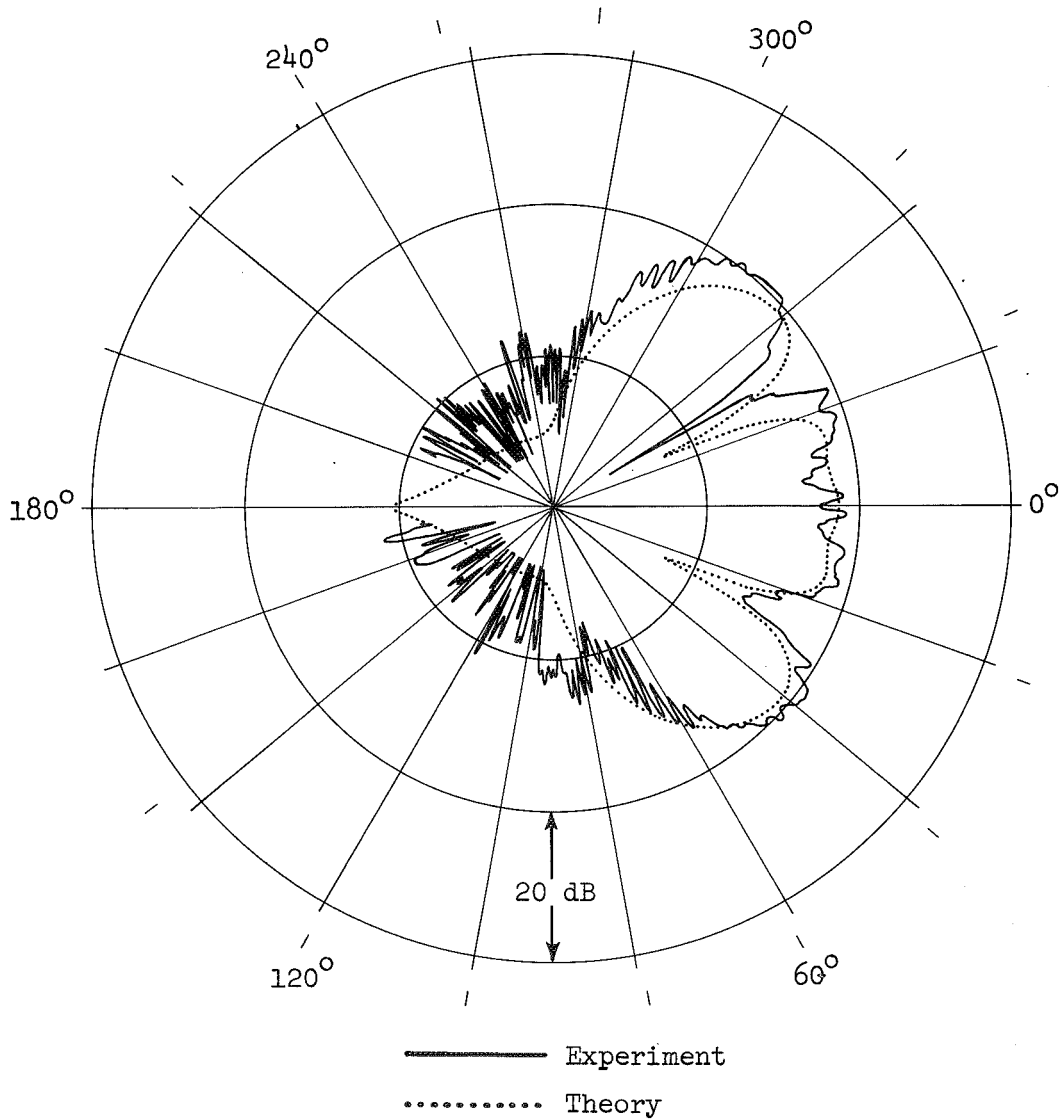


Figure 9.- Radiation patterns at 3776.4 Hz.

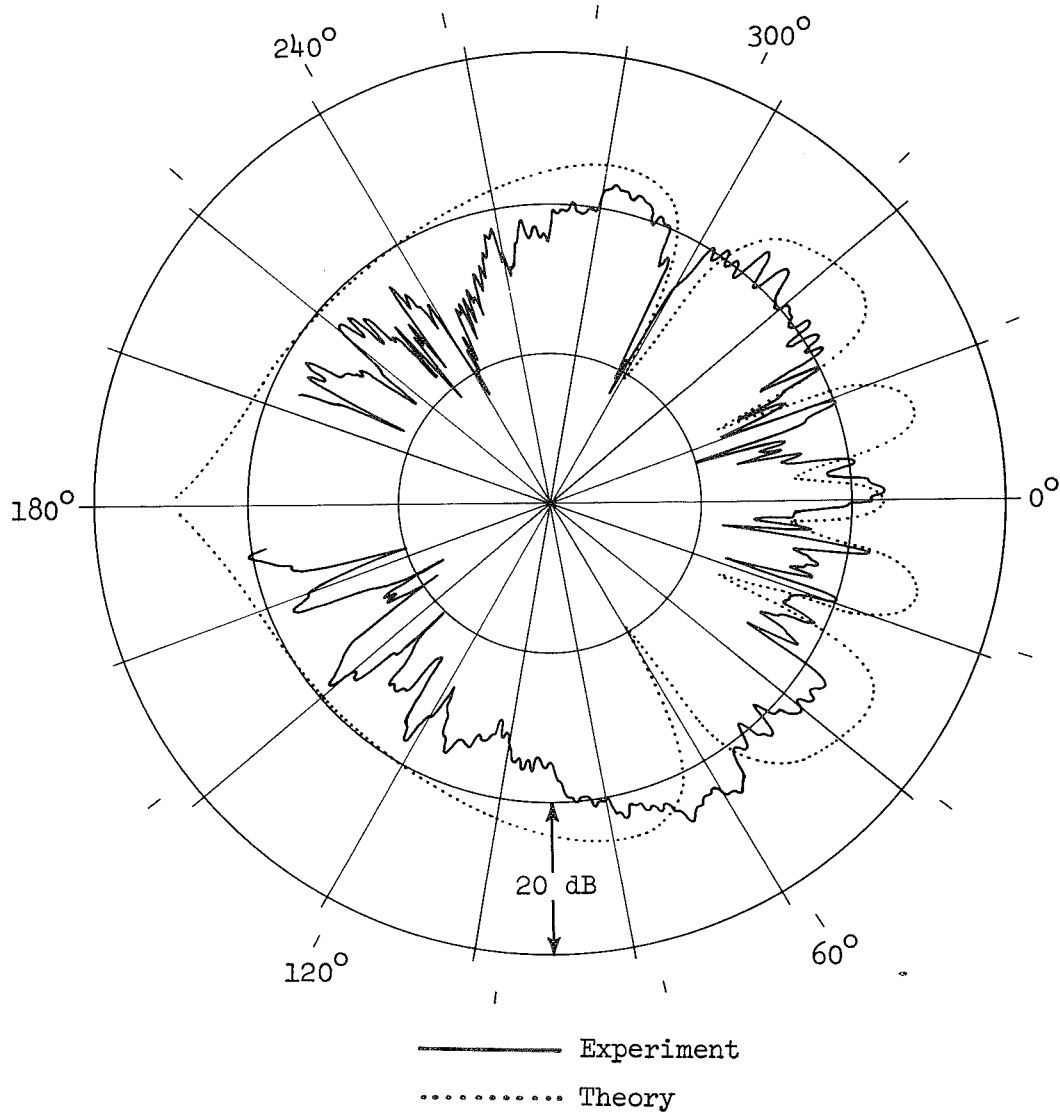
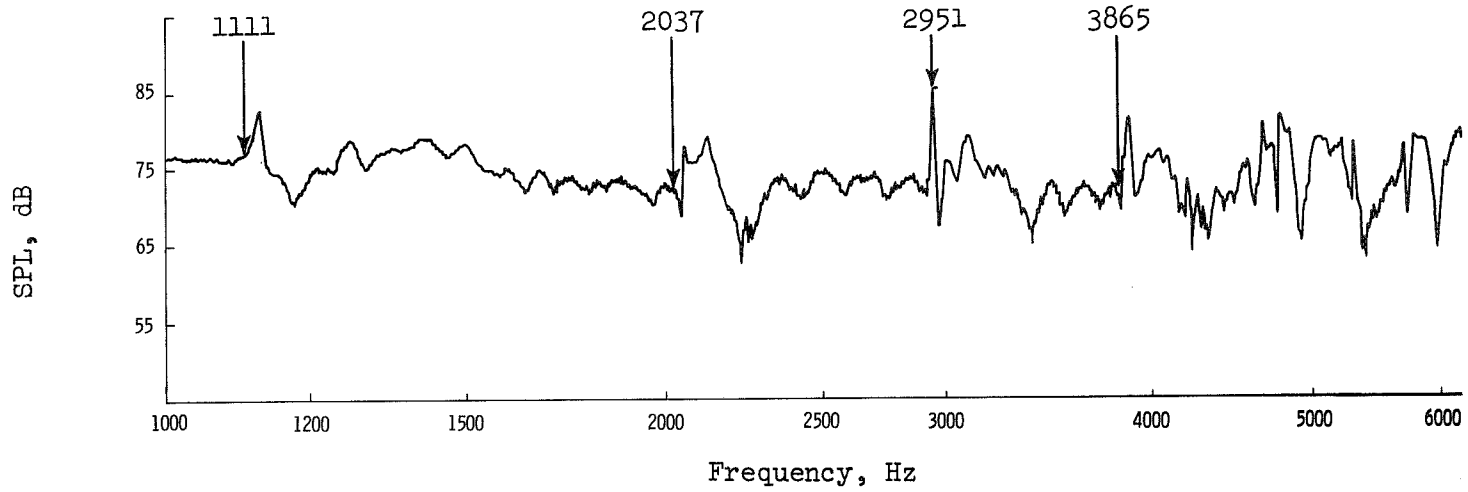
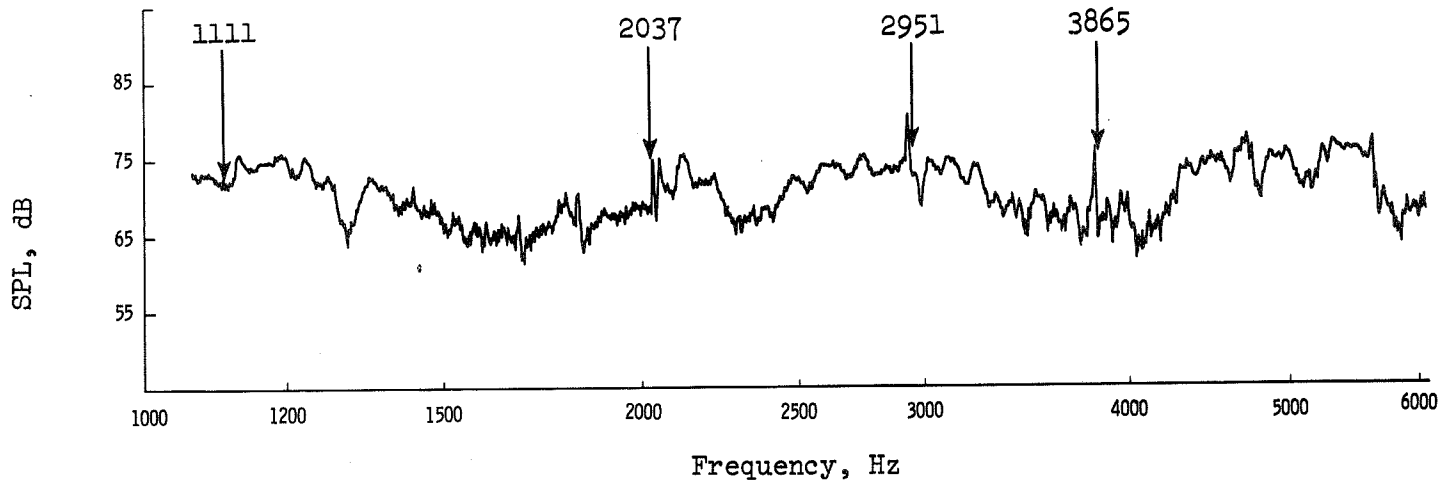


Figure 10.- Radiation patterns at 3897.3 Hz.

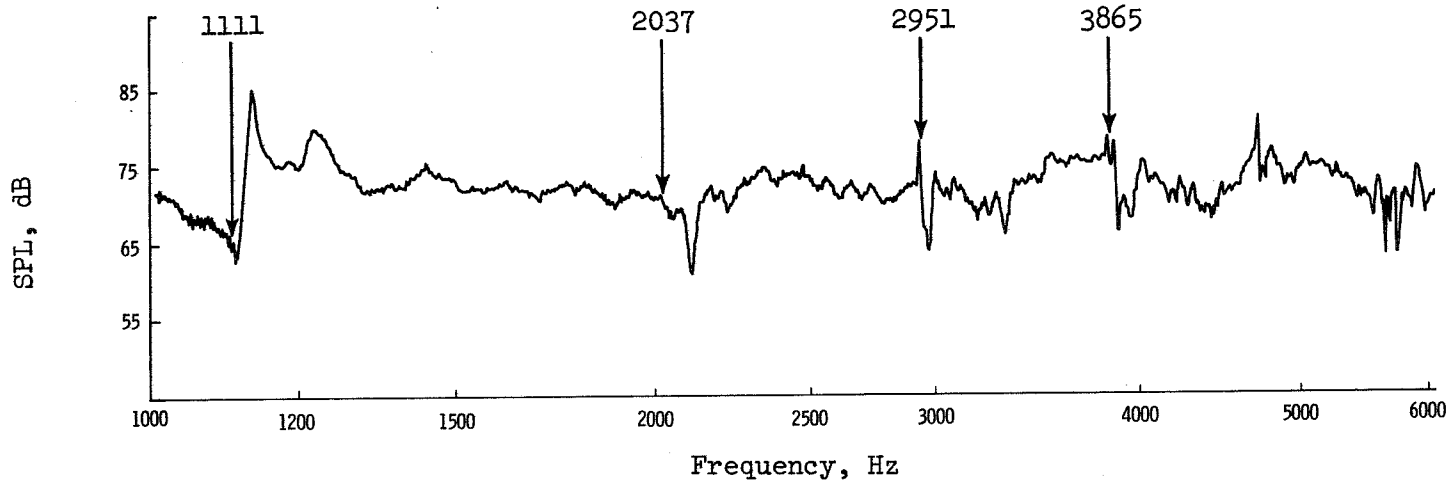


(a) Sweep at 0°.

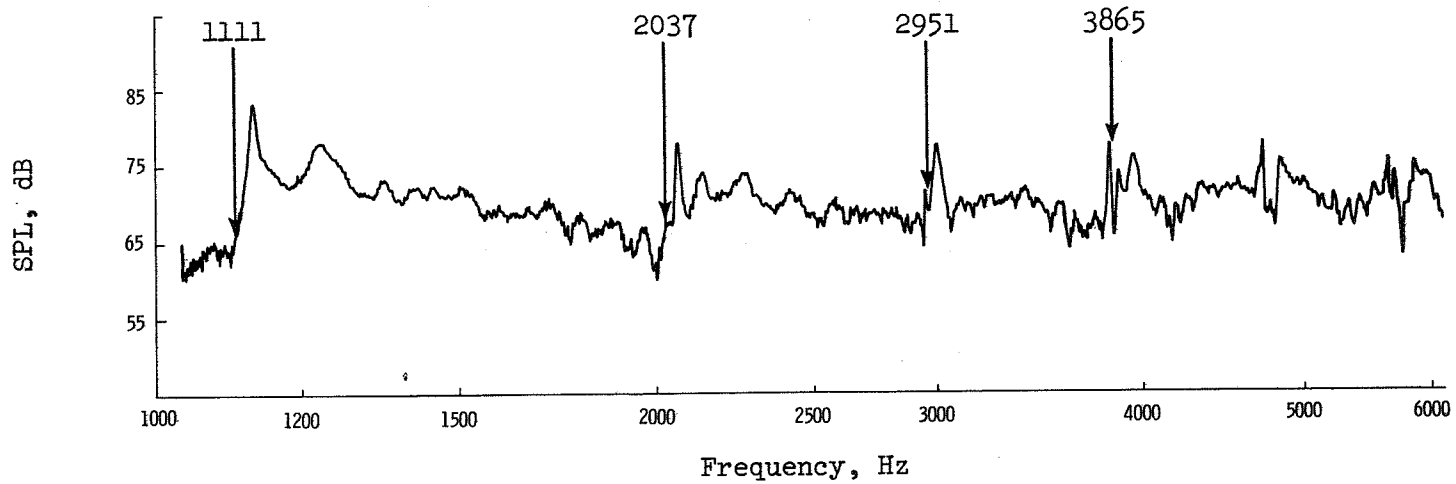


(b) Sweep at 20°.

Figure 11.- Radiated SPL during frequency sweeps.

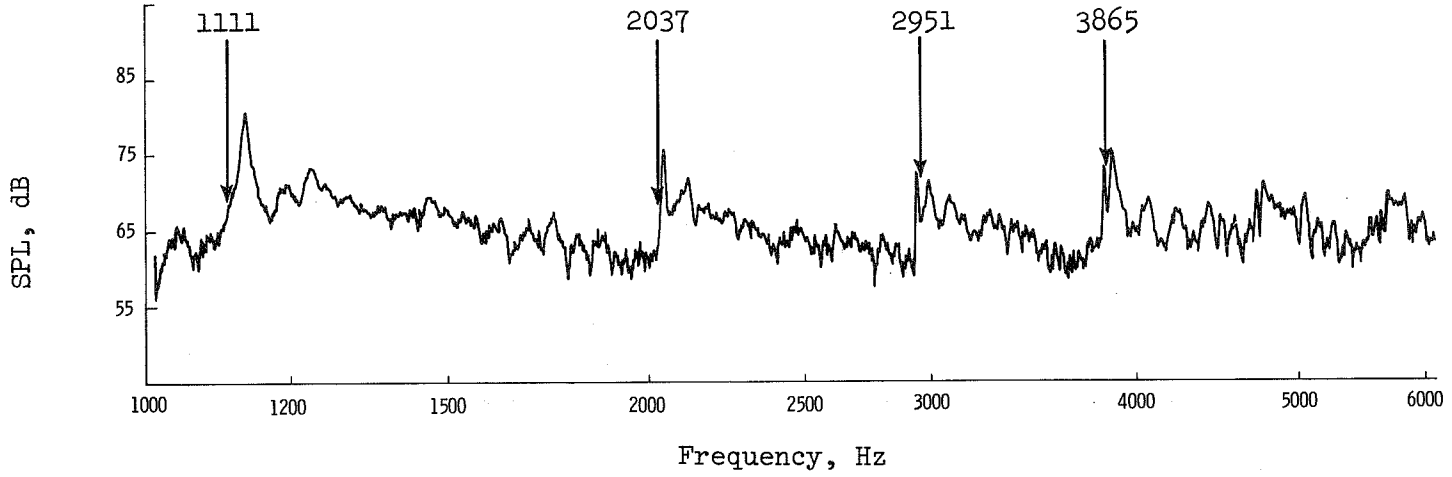


(c) Sweep at 40°.

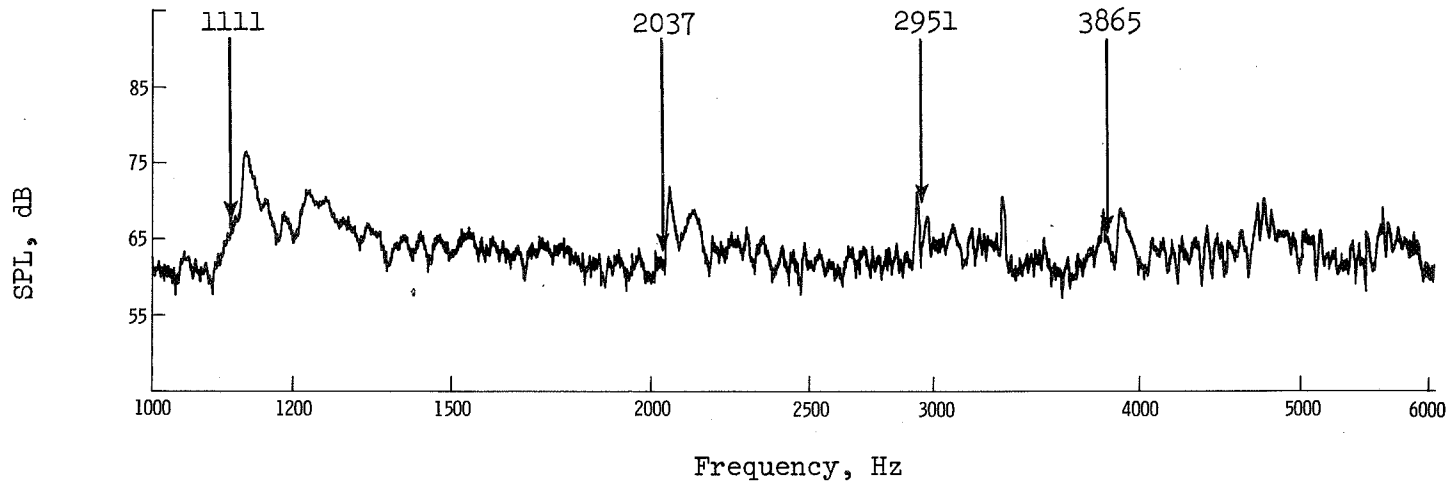


(d) Sweep at 60°.

Figure 11.- Continued.



(e) Sweep at 80°.



(f) Sweep at 100°.

Figure 11.- Concluded.